Journal of Medicinal Chemistry

Article

pubs.acs.org/jmc

Substituted 7-Amino-5-thio-thiazolo[4,5-*d*]pyrimidines as Potent and Selective Antagonists of the Fractalkine Receptor (CX_3CR1)

Sofia Karlström,*[,†] Gunnar Nordvall,[†] Daniel Sohn,[†] Andreas Hettman,[†] Dominika Turek,[†] Kristofer Åhlin,[†] Annika Kers,[†] Martina Claesson,[†] Can Slivo,[†] Yvonne Lo-Alfredsson,[†] Carl Petersson,[†] Galina Bessidskaia,[†] Per H. Svensson,[‡] Tobias Rein,[‡] Eva Jerning,[†] Åsa Malmberg,[†] Charlotte Ahlgen,[†] Colin Ray,[†] Lauri Vares,[†] Vladimir Ivanov,[†] and Rolf Johansson*[,†]

[†]CNSP iMed Science Södertälje, AstraZeneca Research and Development, Innovative Medicines, SE-15185 Södertälje, Sweden

[‡]Pharmaceutical Development, AstraZeneca Research and Development, SE-15185 Södertälje, Sweden

Supporting Information

ABSTRACT: We have developed two parallel series, A and B, of CX_3CR1 antagonists for the treatment of multiple sclerosis. By modifying the substituents on the 7-amino-5-thio-thiazolo[4,5-*d*]-pyrimidine core structure, we were able to achieve compounds with high selectivity for CX_3CR1 over the closely related CXCR2 receptor. The structure−activity relationships showed that a leucinol moiety attached to the core-structure in the 7-position together with *α*-methyl branched benzyl derivatives in the 5-position displayed promising affinity, and selectivity as well as physicochemical properties, as exemplified by compounds **18a** and **24h**. We show the preparation of the first potent and selective orally available CX_3CR1 antagonists.

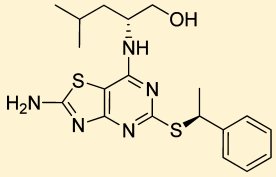

18a
Series A

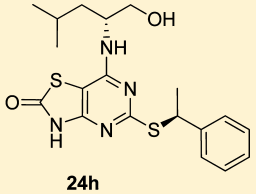

24h
Series B

INTRODUCTION

Fractalkine (FKN, CX_3CL1), the sole member of the CX_3C family (*δ*-family) of chemokines, is a 355 amino acid peptide that activates the heptahelical CX_3CR1.[1] FKN is unique among the chemokines in the respect that it is formed as a membrane bound peptide that is subsequently cleaved by proteases such as ADAM17 (ADAM metallopeptidase domain 17, also known as tumor necrosis factor-*α*-converting enzyme (TACE)) and ADAM10[2] and cathepsin S,[3] leaving a pharmacologically soluble and active peptide/chemokine. The chemokine distribution is widespread and is also regulated by environmental factors such as inflammation.[4]

CX_3CR1 is expressed in the brain, spleen, and in subpopulations of leukocytes such as monocytes, macrophages, and microglia,[5] cells of monocytic lineage such as osteoclasts and dendritic cells, and neutrophils but also in lymphocytes such as the T-cell and the NK-cell. In the lymphocyte, high expression is found in cytotoxic cells such as the NK-cell (natural killer cell), *γδ*-T cells, and CD8+ (cluster of differentiation 8+) cells.[6] In monocytes, CX_3CR1 is highly expressed in cells also having high expression of the scavenger receptor CD16 (Fc*γ*RIII). This subset of monocytes, CD14+CD16+ cells, which corresponds to 5−15% of the total peripheral blood monocyte population,[7] have attracted attention because they are expanded in diverse inflammatory diseases such as atherosclerosis, rheumatoid arthritis,[8] and infective disorders[6,9] as well as in other pathologies like cancer.[6]

Monocytes/macrophages and lymphocytes are key players in the pathology of inflammatory diseases. By a sustained influx from the blood into the surrounding tissue, these cells contribute to the chronicity of tissue damage and organ dysfunction through phagocytosis and production of cytotoxic species. Interestingly, corticosteroids selectively suppress the CD14+CD16+ subpopulation of monocytes in the blood during the treatment of multiple sclerosis (MS)[10] and inflammatory bowel disease (IBD).[11]

The exact mechanism of the diapedesis is complex and far from completely understood. Key elements are the chemotactic activity of the chemokine[12] as well as the ability to strongly adhere to the luminal wall under high shear force.[13] Still, a number of other events are required in order for cells to make their way into the surrounding tissue.[14]

The CX_3CR1 receptor is of interest for the role in migration and adhesion[15] and hence the inhibition of extravasation of proinflammatory lymphocytes and leukocytes, and antagonists of FKN induced events is potentially an attractive approach to the treatment of inflammatory diseases.[16]

Chemokine receptors are G-protein coupled receptors, which are generally regarded as druggable targets with a good feasibility for identification of antagonists.[17] A number of antagonists of the CCR (CC chemokine receptor)[18−21] and CXC[22,23] family of receptors have previously been identified through HTS (high throughput screening) campaigns, and we were surprised that our initial high throughput screen of 150 K compounds did not produce any productive hit series against the CX_3CR1 receptor. We therefore turned our attention to a more focused screening effort. By testing a small collection of

Received: August 29, 2012
Published: March 21, 2013

dx.doi.org/10.1021/jm3012273 | *J. Med. Chem.* 2013, 56, 3177−3190

about 1000 compounds from other in-house projects targeting chemokine receptors, we identified compounds **1**–**4** as suitable starting points for the development of potent and selective CX_3CR1 antagonists.[24]

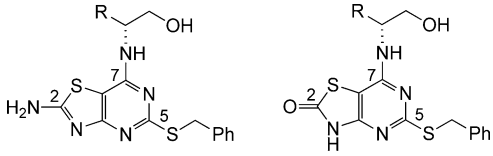

1 R = Me
2 R = Et
Series A

3 R = Me
4 R = Et
Series B

CHEMISTRY

To find potent and CX_3CR1 selective compounds, we designed a synthetic strategy that allowed the systematic variation of the 5- and 7-substituents on the scaffolds represented by compounds **1**–**4**. The synthesis of the 2-aminosubstituted analogues is outlined in Scheme 1. Commercially available compound **5** was treated with sodium hydride and benzyl bromide to give compound **6**. Electrophilic addition of thiocyanate followed by condensation at elevated temperatures afforded the thiazole **8**. The 7-hydroxy group was then converted in a Vilsmeier reaction to the corresponding chloride **9** to introduce a good leaving group. The chloride was subsequently displaced in a nucleophilic aromatic substitution reaction to allow the introduction of a variety of aminoalcohols **10** to give compounds **11** (Table 1). By choosing an enantiomerically pure aminoalcohol, a single enantiomer of compound **11** was obtained without any racemization.

To obtain compound **11f**, the required aminoalcohol was prepared and coupled with compound **9** as described in Scheme 2.

The 5-position was accessed by the removal of the *S*-benzyl group in a Birch reduction[25] of a compound **11** to liberate the free thiol **12a**–**b**, followed by a coupling of the thiol with the appropriate alkylating agent. The easily accessible organic chloride **13** was used to give **14** in a S_N2-type reaction (Scheme 3). To prevent oxidation of the thiol **12** to the corresponding disulfide, a process that occurs relatively fast in DMSO in air, it was important to run the coupling reaction under an inert atmosphere. Further improvement was seen if the reaction was run in the presence of a reducing agent such as sodium borohydride. In this way any formed disulfide was reduced back to free thiol **12** that could react with the alkylating agent.

Reaction of the branched alkyl halide **17** with **12** gave the branched thioether **18** (Scheme 4). Racemic **17** gave a mixture of diastereomers of compound **18** that could be separated on HPLC using a nonchiral reversed phase column or a straight phase chiral column. Alternatively, the ketones (**15**) were enantioselectively reduced by (−)-B-chlorodiisopinocampheylborane (DIPCl)[26] or using a method employing (*R*)-(+)-α,α-diphenyl(pyrrolidin-2-yl)methanol borate complex and borane methyl sulfide as reducing agent[27] to give the (*S*)-alcohols **16**. Employing the opposite reagent of the chiral reagent gave *R*-**16**. Alcohols **16** were then converted to the chlorides **17** with mainly inversion of configuration by methods employing for example NCS (*N*-chlorosuccinimide) and triphenylphosphine, or cyanuric chloride and DMF (Scheme 4). Reaction of enantiomerically pure or enriched **17** with the thiol **12** proceeded with inversion of configuration resulting in a net retention of configuration from **16** to **18**. High diastereomeric purity of compounds **18** could be obtained via this sequence combined with chromatographic purification.

The thiazolonopyrimidines were derived from the corresponding compounds **11**, **14**, or **18** by the method shown in Scheme 5. A Sandmeyer-type reaction converted the 2-amino group into the 2-chlorothiazole **19** or **22**. The chloride was subsequently transformed into a methoxy-group in **20** or **23** that finally was hydrolyzed to yield compounds **21** and **24**.

To allow for a later stage introduction of the 5-position substituent, the method outlined in Scheme 6 was developed. The thiol **12** was oxidized to the disulfide **25** under the Sandmayer conditions employed in the conversion of the 2-amino group into a 2-chloro substituent. The dimeric compound was then taken through the steps previously described for the synthesis of **24** (Scheme 5) to yield the dimer **27**. Dimer **27** was reduced back to thiol **28** by addition of a stoichiometric amount of $NaBH_4$. The formed thiol was then reacted with the halide **17** in situ to give compound **24**.

To unambiguously verify the configuration of the stereocenters in the purified diastereomers, compound **18a** (Figure 1, left) and compound **24h** (Figure 1, right) were subjected to crystallization and X-ray structure investigation. Crystals of **18a**·HCl were obtained by crystallization from MeOH/EtOAc and the derived X-ray structure demonstrates the 5*S*/7*R* config-

Scheme 1. Synthesis of 2-Aminosubstituted Analogues 11

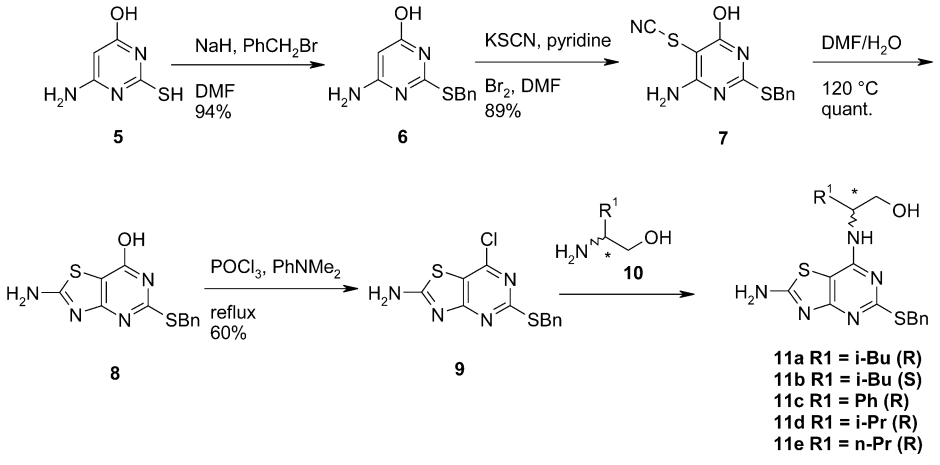

dx.doi.org/10.1021/jm3012273 | J. Med. Chem. 2013, 56, 3177−3190

Scheme 2. Synthesis of Compound 11f

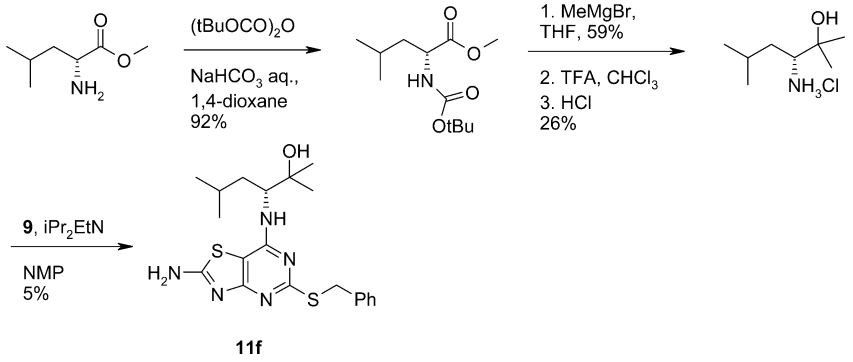

Scheme 3. Synthesis of Compounds 14

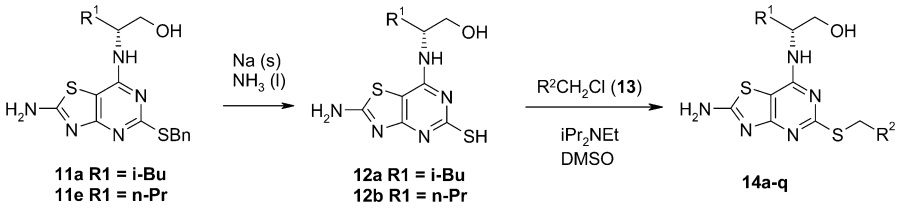

Scheme 4. Synthesis of Compounds 18

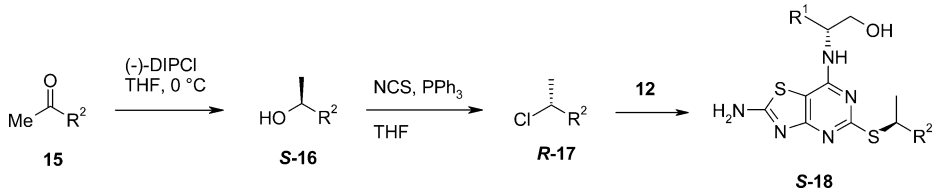

Scheme 5. Synthesis of [1,3]Thiazolo[4,5-*d*]pyrimidin-2(3*H*)-ones 21 and 24

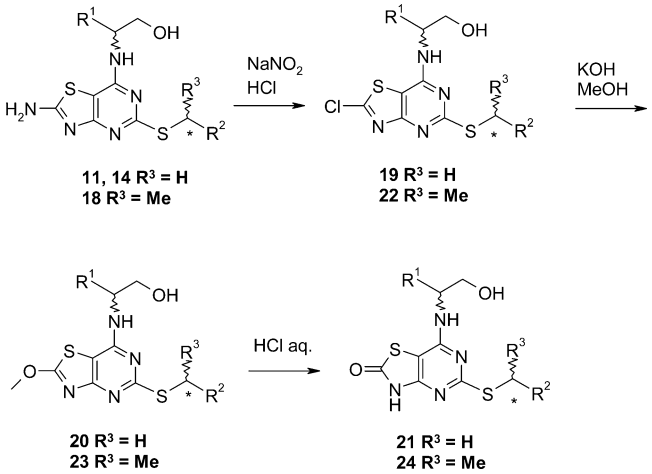

uration. Compound **24h** was crystallized from MeOH as a hemihydrate. The obtained structure also verifies the configuration of the stereocenters.

We also made the corresponding sulfone and sulfoxide **29** and **30** from compound **21a** via oxidation with oxone, either >2 equiv or 1 equiv, respectively. Compound **31** containing an ether instead of thioether was prepared by employing the sulfone in compound **29** as leaving group in a reaction with benzyl alcohol as shown in Scheme 7.

RESULTS AND DISCUSSION

Exploring the 7-Substituent. The initial hit compounds **2** and **4** containing a 2-ethyl-2-aminoalcohol were more potent than the corresponding alaninol derivatives **1** and **3**, indicating that the lipophilicity of the amino alcohol side chain was of importance for affinity. Thus, we decided to introduce a range of lipophilic groups in this position while retaining the alcohol moiety. The derived compounds were tested in a CX_3CR1 receptor binding assays using [^{125}I]-fractalkine as the radioligand. The hits originated from an in-house CXCR2 antagonist program and displayed high affinity for this receptor. Because our aim was to develop a selective CX3CR1 antagonist, we also included a CXCR2 receptor binding assay, using [^{125}I]-IL8 as the radioligand, as a selectivity assay in the screening cascade.[24c] The assay results together with the selectivity for the compounds for the CX_3CR1 receptor over the CXCR2 receptor (the ratio: $K_i(CX_3CR1/K_i(CXCR2))$ are summarized in Table 1. By replacing the R^1 methyl group in compound **1** with an ethyl (compound **2**) or an isopropyl group (compound **11d**), potency increased marginally, whereas larger groups such as a *n*-propyl as in **11e** and the isobutyl derivative **11a** resulted in a significant increase in potency. Generally, it appears that the more lipophilic the moiety in this region is, the more potent the compound is at the CX_3CR1 receptor. Compounds containing both enantiomers of the leucinol chain were prepared and tested (*R*-**11a** and *S*-**11b**), which showed that the *R*-enantiomer is highly preferred over the *S*-enantiomer for binding to the CX_3CR1 receptor. This is the same preferred enantiomer as what has previously been reported for the

dx.doi.org/10.1021/jm3012273 | J. Med. Chem. 2013, 56, 3177−3190

Scheme 6. Alternative Method for Synthesis of Compound 24

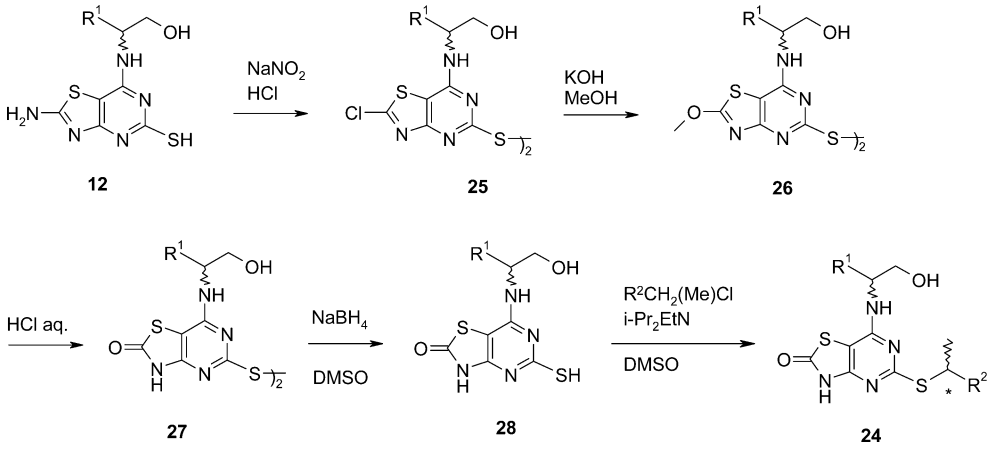

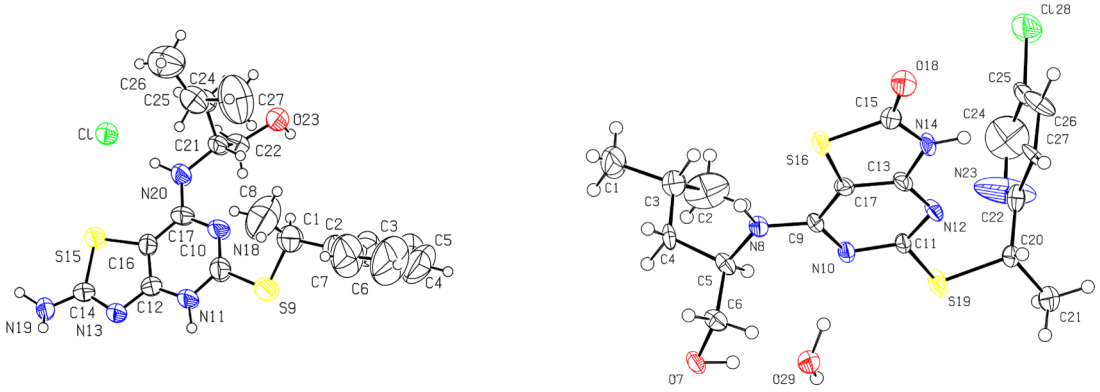

Figure 1. Crystal structures of compounds **18a**-HCl and **24h**-H_2O.

Scheme 7. Synthesis of Compounds 29, 30, and 31

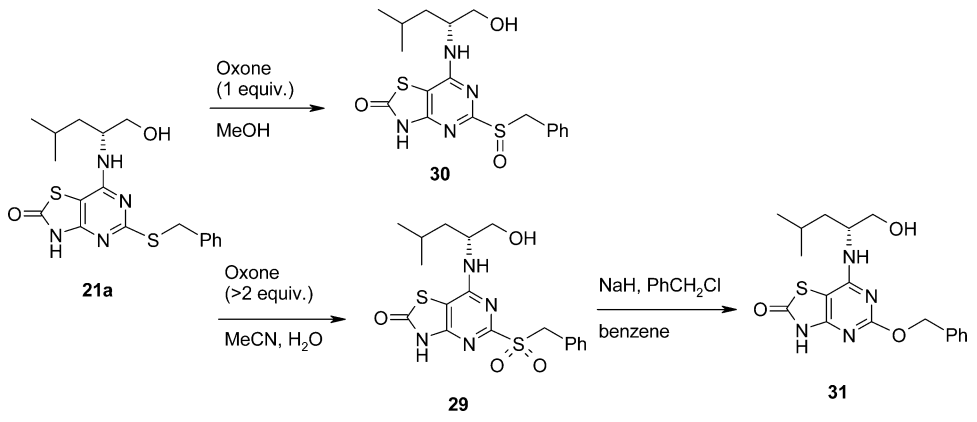

CXCR2-antagonists.[24a,b] The phenyl derivative **11c** show similar potency compared to the *t*-Bu derivative **11g**, indicating that also the shape and length of the R^1-subtituent is of importance for affinity. A larger R^1-group not only increases CX_3CR1 affinity but also decrease the affinity for the CXCR2 receptor as can be concluded from the data in Table 1. This observation is in accordance with what has been previously published regarding the SAR (structure−activity relationship) of thiazolopyrimidines targeting the CXCR2 receptor[24a−c] and gives an opportunity to obtain CX_3CR1 selectivity approximately 10-fold over CXCR2, but we reasoned that further optimization was needed to increase selectivity. The thiazolonopyrimidines (series B) analogue **21a** of the most potent aminothiazolopyrimidines **11a** displayed similar CX_3CR1 affinity but significantly higher CXCR2 affinity.

Exploring the 5-Substituent. After the identification of (*R*)-leucinol as a potent and preferable group in the 7-position of the 2-amino-thiazolo[4,5-*d*]pyrimidine core, our attention focused on modification of the *S*-benzyl group in the 5-position. We introduced a range of hydrophilic and lipophilic substituents in the 2, 3, and 4 position of the phenyl ring and also replaced it with the different regioisomers of pyridine (compounds **14**, Table 2). In general, lipophilic substituents in all three positions of the phenyl ring were tolerated whereas the more hydrophilic cyano group resulted in a 2−3-fold reduction in potency in the 2- (compound **14e**) and 3-positions

dx.doi.org/10.1021/jm3012273 | J. Med. Chem. 2013, 56, 3177−3190

Table 1. In Vitro Pharmacological Results of 7-Substituted Aminoalcohol Derivatives

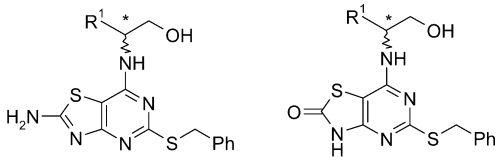

Series A Series B

compd	series	R^1	absolute configuration (*)	CX_3CR1^a	$CXCR2^b$	ratio[c]
1	A	Me	*R*	1100 ± 220	13[d]	0.01
2	A	Et	*R*	770 ± 100	160 ± 4	0.2
3	B	Me	*R*	29000	4.5[d]	0.0002
4	B	Et	*R*	560 ± 50	21 ± 6	0.04
11a	A	*i*-Bu	*R*	48 ± 6	530	11
11b	A	*i*-Bu	*S*	600 ± 70	not tested	
11c	A	Ph	*R*	220 ± 20	not tested	
11d	A	*i*-Pr	*R*	640 ± 60	150 ± 30	0.2
11e	A	Pr	*R*	100 ± 3	510 ± 120	5
11g	A	*t*-Bu	*R*	190 ± 20	370 ± 140	2
21a	B	*i*-Bu	*R*	30 ± 10	79 ± 9	3

[a]Displacement of specific [^{125}I]-CX_3CL1 ([^{125}I]-fractalkine) binding to membrane preparations from HEK293S cells stably expressing human CX_3CR1, expressed as K_i ± SEM (nM). [b]Displacement of specific [^{125}I]-IL8 binding to membrane preparations from HEK293 cells stably expressing human CXCR2, expressed as K_i ± SEM (nM). [c]Ratio of K_i (CXCR2)/K_i (CX_3CR1) [d]IC_{50} (nM) taken from ref 24c.

Table 2. In Vitro Pharmacological Results of Benzyl Substituted Derivatives

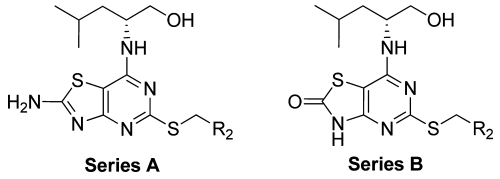

Series A Series B

compd	series	R^2	CX_3CR1^a	$CXCR2^b$	ratio[c]
14a	A	2-Br-phenyl	4.0 ± 2.7	1750 ± 140	435
14b	A	2-Cl-phenyl	51	1790 ± 50	35
14c	A	2-F-phenyl	23 ± 10	220 ± 32	10
14d	A	2-Me-phenyl	70 ± 2.0	1500[d]	21
14e	A	2-CN-phenyl	120 ± 10	4100 ± 570	35
14f	A	2-MeO-phenyl	99 ± 27	590	6
14g	A	3-Br-phenyl	32 ± 10	190	6
14h	A	3-CN-phenyl	91 ± 53	1980 ± 100	22
14i	A	4-Br-phenyl	47 ± 36	1600 ± 130	34
14j	A	4-CN-phenyl	1200 ± 900	258	0.2
14k	A	2-F,4-Br-phenyl	8.1 ± 0.5	567	70
14l	A	2,3-diF-phenyl	71 ± 26	79 ± 20	1
21b	B	2,3-diF-phenyl	10 ± 3.7	4.1 ± 1.6	0.4
14m	A	2-pyridyl	360 ± 10	64	0.2
14n	A	3-pyridyl	670 ± 440	5400 ± 300	8
14o	A	4-pyridyl	900 ± 130	9000 ± 1500	10

[a]Displacement of specific [^{125}I]-CX_3CL1 ([^{125}I]-fractalkine) binding to membrane preparations from HEK293S cells stably expressing human CX_3CR1, expressed as K_i ± SEM (nM). [b]Displacement of specific [^{125}I]-IL8 binding to membrane preparations from HEK293 cells stably expressing human CXCR2, expressed as K_i ± SEM (nM). [c]Ratio of K_i (CXCR2)/K_i (CX_3CR1). [d]*n* = 1.

(compound **14h**) and a 25-fold reduction in potency in the *para*-position (compound **14j**). Thus, the *para*-position appears to be directed toward a more lipophilic region of the receptor. The 2-position appeared to be the most promising region for substitution. The 2-Br derivative **14a** displayed a 12-fold increase in affinity compared to the unsubstituted compound **11a**. In addition, the affinity for the CXCR2 receptor was significantly reduced for several 2-substituted compounds, thus increasing selectivity.

Thus, it appears that a favorable lipophilic pocket exists in the CX_3CR1 receptor but not in the CXCR2 receptor and that this pocket can be accessed from the *ortho* position of the aromatic ring. However, this increase in potency and selectivity was achieved by an increase in lipophilicity and, consequently, low solubility remained an issue (Table 6). As could be expected, solubility was enhanced by the introduction of a pyridine moiety as R^2 as in **14m**, but CX_3CR1 potency was greatly reduced for compounds **14m−o**. We hypothesized that the lipophilic pocket in the CX_3CR1 receptor could also be reached by a substituent from the benzylic position of the linker in the 5-position and that this alternative way of reaching this area also could be advantageous for solubility by introducing bulk in an aliphatic part of the molecule. We prepared a number of compounds with methyl substitution on the benzylic carbon with different substitution patterns on the aromatic ring in both series of compounds, **18** and **24** (Table 3). The branched benzyl moiety gave a further increase of CX_3CR1 activity and selectivity toward CXCR2 than what could be achieved by varying the substituent pattern on the aromatic ring in the *S*-benzyl in the 5-position of the molecule (Table 2). Interestingly, an additional increase in potency for CX_3CR1 or selectivity versus CXCR2 was not achieved for compound **18c** compared to **14a.** Thus, a lipophilic 2-aryl substituent and a branched methyl group on the linker do not show any additive effects, indicating that they may be interchangeable and occupy the same small lipophilic area. In series A, the preferred stereoisomer has the (*S*)-configuration, which has about 4−8 fold higher potency for the CX_3CR1 receptor, whereas the CXCR2 potency is similar between the stereoisomers. Interestingly, for compound **24a** and **24b** from the series B, no preference between stereoisomers is seen for the CX_3CR1 affinity but a 6-fold difference is observed in CXCR2 affinity, leading to the (*R*)-isomer being the most selective. In addition,

dx.doi.org/10.1021/jm3012273 | J. Med. Chem. 2013, 56, 3177−3190

Table 3. In Vitro Pharmacological Results of Methyl Substituted Derivatives

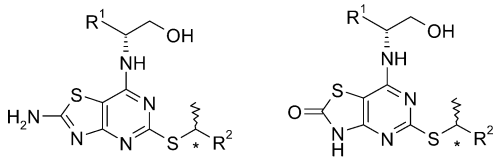

Series A Series B

compd	series	R^1	R^2	absolute configuration (*)	CX_3CR1^a	$CXCR2^b$	ratio[c]
18a	A	*i*-Bu	Ph	*S*	3.9 ± 0.0	2800 ± 340	720
18b	A	*i*-Bu	Ph	*R*	18 ± 3.3	2100 ± 180	120
24a	B	*i*-Bu	Ph	*S*	7.8 ± 1.9	210 ± 60	30
24b	B	*i*-Bu	Ph	*R*	8.0 ± 2.4	1360 ± 30	170
18c	A	*i*-Bu	2-Br-phenyl	*S*	13 ± 2.5	2600 ± 200	200
18d	A	*i*-Bu	2-Br-phenyl	*R*	102 ± 1	6000 ± 1200	60
18e	A	*i*-Bu	2-F-phenyl	*S*	4.7 ± 0.6	1400 ± 530	300
18f	A	*n*-Pr	3-CN-phenyl	*S*	42 ± 21	13000 ± 2000	310
24f	B	*n*-Pr	3-CN-phenyl	*S*	14 ± 1	920 ± 20	65
18g	A	*i*-Bu	3-SO_2Me-phenyl	*S*	28 ± 6	>100000	>3500
18h	A	*i*-Bu	4-Cl-2-pyridyl	*S*	6.2 ± 1.3	1129	180
24h	B	*i*-Bu	4-Cl-2-pyridyl	*S*	5.8 ± 0.4	489	80
24i	B	*n*-Pr	4-Cl-3-pyridyl	*S*	21 ± 5	220 ± 110	10

[a]Displacement of specific [^{125}I]-CX_3CL1 ([^{125}I]-fractalkine) binding to membrane preparations from HEK293S cells stably expressing human CX_3CR1, expressed as K_i ± SEM (nM). [b]Displacement of specific [^{125}I]-IL8 binding to membrane preparations from HEK293 cells stably expressing human CXCR2, expressed as K_i ± SEM (nM). [c]Ratio of K_i (CXCR2)/K_i (CX_3CR1).

the introduction of a methyl group in the benzylic position had a positive effect on solubility (Table 6).

Exploring Linkers. Increasing the 5-position linker length by one additional carbon (compound **14p**) in the substituted aminothiazolo[4,5-*d*]pyrimidines series gave a moderate enhancement of CX_3CR1 activity and retained selectivity toward CXCR2 compared to **11a** (Table 4). A further increase in distance between the core and the aromatic ring gives reduced CX_3CR1-affinity (compound **14q**). The oxidation of the sulfur in **21a** to the sulfone **29** and sulfoxide **30** reduced the affinity for CX_3CR1 about 4−10-fold, indicating that a polar group in this position is not favorable. However, exchanging the thioether in compound **21a** for an ether as in compound **31** leads to retained CX_3CR1 potency and an approximately 4-fold increased selectivity toward CXCR2.

Exploring the Alcohol Group. Coupling of compound **9** with other amino acid derivatives and functional group transformations gave rise to compounds **11f** and **32**−**36** (Table 5). We explored the importance of the alcohol moiety in the 7-position by varying the position and hydrogen bond donating/accepting properties. Extending the alcohol moiety by an additional methylene group (**32**) gave only a small decrease in CX_3CR1 affinity compared to compound **11a**. A significant

Table 4. In Vitro Pharmacological Results of Derivatives with Modified Aryl Linkers

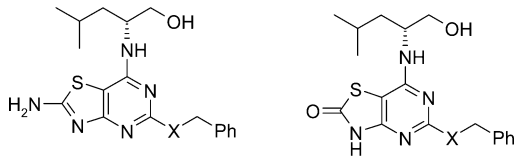

Series A Series B

compd	series	X	CX_3CR1^a	$CXCR2^b$	ratio[c]
14p	A	SCH_2	18 ± 4.0	349	20
14q	A	$S(CH_2)_2$	110 ± 20	523	5
29	B	SO_2	110 ± 24	100 ± 29	0.9
30	B	S(O)	280 ± 28	460 ± 160	1.6
31	B	O	44 ± 7.0	580 ± 56	13

[a]Displacement of specific [^{125}I]-CX_3CL1 ([^{125}I]-fractalkine) binding to membrane preparations from HEK293S cells stably expressing human CX_3CR1, expressed as K_i ± SEM (nM). [b]Displacement of specific [^{125}I]-IL8 binding to membrane preparations from HEK293 cells stably expressing human CXCR2, expressed as K_i ± SEM (nM). [c]Ratio of K_i (CXCR2)/K_i (CX_3CR1).

Table 5. In Vitro Pharmacological Results of Derivatives Modified in the Aminoalcohol Part

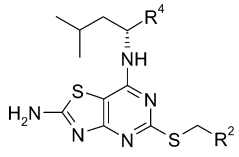

series A

compd	R^2	R^4	CX_3CR1^a	$CXCR2^b$	ratio[c]
11f	Ph	$C(CH_3)_2OH$	1200 ± 300	not tested	
32	2-Cl-phenyl	$(CH_2)_2OH$	91 ± 15	not tested	
33	2-Cl-phenyl	C(O)OMe	43 ± 5	4200 ± 500	100
34	Ph	C(O)OMe	8.3 ± 0.8	1940 ± 200	230
35	Ph	$C(O)NH_2$	220 ± 1	2400 ± 100	11
36	Ph	C(O)OH	320 ± 15	5900 ± 800	20

[a]Displacement of specific [^{125}I]-CX_3CL1 ([^{125}I]-fractalkine) binding to membrane preparations from HEK293S cells stably expressing human CX_3CR1, expressed as K_i ± SEM (nM). [b]Displacement of specific [^{125}I]-IL8 binding to membrane preparations from HEK293 cells stably expressing human CXCR2, expressed as K_i ± SEM (nM). [c]Ratio of K_i (CXCR2)/ K_i (CX_3CR1).

dx.doi.org/10.1021/jm3012273 | *J. Med. Chem.* 2013, 56, 3177−3190

Table 6. Solubility, Cl_{int} in Human Microsomes, and Caco-2 Permeability of Selected Compounds

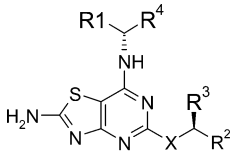

Series A

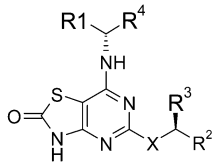

Series B

compd	series	X	R^1	R^2	R^3	R^4	solubility[a]	Cl_{int}[b]	Caco-2 A–B P_{app}[c]
11a	A	S	*i*-Bu	Ph	H	CH_2OH	<1	ND	ND
11e	A	S	*n*-Pr	Ph	H	CH_2OH	19	23	6
11g	A	S	*t*-Bu	Ph	H	CH_2OH	11	17	8
14a	A	S	*i*-Bu	2-Br-phenyl	H	CH_2OH	3	48	ND
14b	A	S	*i*-Bu	2-Cl-phenyl	H	CH_2OH	<1	ND	ND
14e	A	S	*i*-Bu	2-CN-phenyl	H	CH_2OH	3	ND	ND
14i	A	S	*i*-Bu	4-Br-phenyl	H	CH_2OH	<1	ND	ND
14m	A	S	*i*-Bu	2-pyridyl	H	CH_2OH	>100	99	1.6
18a	A	S	*i*-Bu	Ph	Me	CH_2OH	22	34	high[d]
18h	A	S	*i*-Bu	4-Cl-2-pyridyl	Me	CH_2OH	63	81	1
21a	B	S	*i*-Bu	Ph	H	CH_2OH	1	ND	ND
24a	B	S	*i*-Bu	Ph	Me	CH_2OH	34	46	20
24h	B	S	*i*-Bu	4-Cl-2-pyridyl	Me	CH_2OH	79	77	>33
29	B	SO_2	*i*-Bu	Ph	H	CH_2OH	>100	ND	1
30	B	SO	*i*-Bu	Ph	H	CH_2OH	>100	4	1
31	B	O	*i*-Bu	Ph	H	CH_2OH	79	67	23
33	A	S	*i*-Bu	2-Cl-Ph	H	C(O)OMe	<1	ND	ND
35	A	S	*i*-Bu	Ph	H	$C(O)NH_2$	10	62	ND
36	A	S	*i*-Bu	Ph	H	C(O)OH	>100	1	ND

[a]HT solubility (μM). [b]In vitro metabolic stability in human microsomes (μL/min/mg). [c]Permeability P_{app} (apparent permeability coefficient) A–B in Caco-2 cells at pH 6.5 (10^{-6} cm/s). [d]A permeability value could not be reported due to low recovery of the compound in the experiments.

decrease in CX_3CR1 affinity was seen for the tertiary dimethylalcohol **11f**, thus the receptor interaction is sensitive to increasing the steric bulk in this area. The hydrogen bond donating ability of the alcohol does not appear to be essential for activity because compounds **33** and **34** with an ester functionality retained the same potency as the alcohol analogue **14b**. The 4–6-fold reduction in potency seen for the carboxamide **35** and carboxylic acid **36** could be due to higher polarity and hence higher desolvation energy penalty. Thus, there is an apparent need for an acceptor but not for a donor moiety, however, the replacement of the alcohol with an ester did not improve solubility (Table 6).

DMPK Properties. Table 6 displays solubility, metabolic stability in human microsomes and Caco-2 permeability data for selected compounds previously discussed in Tables 1–5. Metabolic stability was similar in both series A and B. A trend was observed between molecular weight and metabolic stability, hence the benzyl substituted analogues displayed somewhat increased metabolism in in vitro systems. Compounds with low lipophilicity, for example, compounds **30** and **36**, also showed low metabolic turnover. Studies of metabolic pathways indicated significant contributions of alkylchain oxidation, dealkylation of the benzyl group, and glucuronidation of the free hydroxyl.

The permeability in Caco-2 cells systems was generally high for the acidic series B, whereas the neutral series A showed moderate to poor permeability. For both series, a trend of lower permeability with increased molecular weight was observed, consistent with earlier reported findings.[28] Compound **18a**, a representative for the series A, displayed high potency and good selectivity versus the CXCR2 receptor together with adequate metabolic stability and solubility and high Caco-2 permeability. In series B, compound **24h** was the most potent compound and showed 80-fold selectivity vs CXCR2 and adequate in vitro DMPK properties. These compounds displayed promising in vitro characteristics and were selected for further characterization.

Pharmacokinetics in rodents indicated moderate and low volume of distribution for series A and B, respectively, as exemplified for compounds **18a** and **24h** in Table 7. Clearance

Table 7. Pharmacokinetic Parameters for Compounds 18a and 24h in Rats

compd	CL (mL/min × kg)	$t_{1/2}$ iv (h)	$t_{1/2}$ po (h)	V_{SS} (Lkg^{-1})	*F* (%)
18a	13	1.9	2.7	1.1	39
24h	1.3	5.5	4.0	0.4	78

was moderate and low for series A and B, respectively. These findings are consistent with the expected differences in plasma protein binding between the two ion classes as acids (series B) are known to have higher plasma protein binding than neutrals (series A).[29] The oral bioavailability (*F*%) was acceptable for both series, slightly higher for series B, in line with observed Caco-2 results. For the treatment of MS, the compounds should also preferably access the brain. Permeability results for several of the compounds from an in vitro BBB-model showed low to moderate permeabilities but were inconclusive. However, as discussed below, compound **18a** has nevertheless showed promising results in an in vivo disease model for MS. It should also be kept in mind that the BBB is disrupted in MS-patients.[30]

dx.doi.org/10.1021/jm3012273 | J. Med. Chem. 2013, 56, 3177–3190

Series Properties. The SAR in series A and B is broadly parallel at both the CX_3CR1 and the CXCR2 receptor, indicating that the receptor interactions of the neutral aminothiazole (series A) and acidic 2-thiazolone (series B) are similar despite the fact that they belong to different ion classes. The physicochemical differences between the series are reflected in a generally lower Caco-2 permeability for the neutral series A, probably due to the larger number of hydrogen bond donors/higher PSA. As demonstrated in Table 7, examples from both series show good oral bioavailibility. For both series, the high clogP (>3.5) of many of the compounds presented have negative implications on properties such as solubility (Table 6) and hERG (the human ether-à-go-go-related gene) inhibition (data not shown).

In vitro receptor binding with [^{3}H]**18a** and mechanism studies with [^{125}I] CX_3CL1 indicate that **18a** and FKN binds to separate binding sites on the receptor and thus this compound is an allosteric antagonist. Determination of the mechanism of antagonism was performed using binding experiments with increasing concentrations of [^{125}I]CX_3CL1. The results suggest that compounds in this class inhibit the binding of [^{125}I]-CX_3CL1 to the hCX_3CR1 receptor through a noncompetitive mechanism as the IC_{50} values do not increase with increasing concentration of [^{125}I]CX_3CL1.

Compound **18a** appear to be selective versus other screened receptors including other chemokine receptors. In vitro receptor binding studies showed 246-fold selectivity versus hCCR1 and 187-fold versus hCCR2 and no significant antagonism of the CCR4, CCR5, CCR6, CXCR3, and CXCR5 receptors. Compound **18a** did not show significant interactions with the majority of the targets in a broad screen with 65 different receptors, enzymes, or ion channels (MDS Pharma Services), but a significant interaction (>50% activity at 10 μM) was observed for the adenosine A1 receptor and the selectivity was later determined to be 33-fold (K_i 132 nM). Other interactions were observed with dopamine, norepinephrine, serotonin transporters, and sodium channel site 2, but selectivities were greater than 200-fold.

Further in vitro pharmacological characterization of **18a** included inhibition of fractalkine stimulated GTPγS binding in the low nanomolar range, potent inhibition of human peripheral blood monocyte adhesion to a FKN-coated surface, and potent inhibition of soluble FKN-induced monocyte migration. In addition, FKN-induced actin polymerization was used as an ex vivo biomarker for the functional inhibition of CX_3CR1 by **18a** in whole blood. Compound **18a**, in a concentration-dependent fashion, inhibited FKN-induced actin polymerization in monocytes from human and rat blood. In vivo characterization of **18a** was performed in the rat experimental autoimmune encephalomyelitis (EAE) disease model of MS. Continuous subcutaneous (sc) administration of **18a** has repeatedly shown strong and dose dependent effects in the MOG-induced EAE model. The compound has completely reversed clinical symptoms, and the treatment effect has been confirmed histologically through reduced spinal cord neuroinflammation and demyelination. The calculated effective IC_{50} concentrations in the EAE rats were in the range of 1.5−4 μM (mean 2 μM). The details of the in vitro and in vivo characterization of **18a** will be presented in separate papers currently in preparation.

CONCLUSIONS

We have from a small set of HTS hits originally targeting the CXCR2 receptor developed a number of CX_3CR1 antagonists.[31] Two series with overlapping SAR but different physicochemical properties have been explored. We have extensively explored three areas of the molecules. The aminoalcohol moiety in the 7-position requires a lipophilic region as well as a hydrogen bond acceptor. In the benzyl linker, we discovered that a methyl substituted linker improved selectivity as well as solubility. The aromatic ring in the 5-position was the most tolerable position for introducing polar groups to balance lipophilicity, solubility, and potency. We were able to reduce the CXCR2 affinity and improve the CX_3CR1 affinity of the substance classes. The structure−activity relationships show that a leucinol moiety attached to the core structure in the 7-position together with α-methyl branched benzyl derivatives in the 5-position show promising affinity and selectivity as well as physicochemical properties. Thus, we have prepared the first potent and selective orally available CX_3CR1 antagonists.

EXPERIMENTAL SECTION

Crystal Data for 18a-HCl. $C_{19}H_{25}N_5OS_2{\cdot}HCl$, M_r = 440.0 g/mol, monoclinic, space group $P2_1$ (no. 4), a = 13.913(1) Å, b = 9.156(1) Å, c = 18.750(1) Å, β = 106.85(1)°, V = 2285(3) Å^3, Z = 4, D_{calc} = 1.279 g cm^{-3}, μ(Mo Kα) = 3.69 cm^{-1} R = 0.041, wR^2 = 0.074, GOF = 1.773. The data were collected at 293K on a KappaCCD diffractometer with graphite monochromatized Mo Kα radiation (λ = 0.71073 Å) and employing a 0.02 mm × 0.29 mm × 0.46 mm crystal (6200 unique, R_{int} = 0.03).

Crystal Data for 24h-H_2O. $C_{18}H_{22}ClN_5O_2S_2{\cdot}1/2H_2O$, M_r = 458.0 g/mol, tetragonal, space group $P4_32_12$ (no. 96), a = 10.3691(3) Å, b = 10.3691(3) Å, c = 39.7170(13) Å, V = 4270.2(2) Å^3, Z = 8, D_{calc} = 1.397 g cm^{-3}, μ(Mo Kα) = 4.01 cm^{-1}, R = 0.083, wR^2 = 0.184, GOF = 1.19. The data were collected at 200K on a KappaCCD diffractometer with graphite monochromatized Mo Kα radiation (λ = 0.71073 Å) and employing a 0.09 mm ×0.11 mm × 0.15 mm crystal (3346 unique, R_{int} = 0.051).

CCDC-889652 and CCDC-889653 contains the supplementary crystallographic data for **18a**-HCl and **24h**-H_2O, respectively. These data can be obtained free of charge from The Cambridge Crystallographic Data Centre via www.ccdc.cam.ac.uk/data_request/cif.

Receptor Binding Assays. *Material.* Recombinant human [^{125}I]CX_3CL1 (specific activity 2200 Ci/mmol) was from PerkinElmer, LifeSciences Inc., Boston, MA, USA. Unlabeled recombinant human fractalkine and human CXCL8 (IL8) was purchased from PeproTech EC Ltd. (London, UK). Human embryonic kidney suspension (HEK-293S) cells stably transfected with human CX_3CR1 and cotransfected with Gαqi5 (hCX_3CR1/Gαqi5) were obtained from Molecular Sciences, AstraZeneca R&D Södertälje, Sweden. HEK293-cells stably transfected with hCXCR2 were obtained from AstraZeneca R&D Charnwood. Recombinant human [^{125}I]-IL8 (CXCL8), (spec. activity 2200 Ci/mmol) was from PerkinElmer, LifeSciences Inc., Boston, MA, USA. Wheatgerm Agglutinin (WGA) SPA beads were purchased from Amersham Biosciences, Sweden.

Cell Culture and Membrane Preparation. The hCX_3CR1/Gαqi5 cells were cultured in Dulbecco's Modified Eagle Medium (DMEM) containing Glutamax and supplemented with 10% fetal bovine serum (FBS), 100 U/mL penicillin, and 100 μg/mL streptomycin (PEST). Selection was performed with 250 μg/mL Zeocin and 100 μg/mL hygromycin for hCX_3CR1/Gαqi5. Cells were incubated at 37 °C and 5% CO_2. To avoid reduced receptor expression, the confluence was not allowed to exceed 80%. The cells were detached with 0.05% trypsin and 0.02% EDTA in phosphate-buffered saline (PBS). Cells were rinsed twice with PBS, scraped, and pooled in harvesting buffer (10 mM Tris-HCl, 5 mM EDTA, 0.1 mg/mL Bacitracin, pH 7.4),

followed by centrifugation at 300*g* for 10 min (4 °C). Collected cells were resuspended in harvesting buffer before homogenization using a Dounce homogenizer. The homogenate was centrifuged at 48000*g* for 10 min (4 °C). The pellet was suspended in harvesting buffer, and aliquots were stored at −70 °C. Protein concentration was determined using a modified method by Lowry.[32] Cell membranes were thawed, homogenized using an Ultra-Turrax homogenizer, and diluted in the appropriate buffer on the day of experiment.

HEK293-cells stably transfected with hCXCR2 were cultured in EMEM containing Glutamax and supplemented with 10% FBS (from PAA, Austria), 1% nonessential amino acids (NEAA), 100 U/ml penicillin, and 100 μg/mL streptomycin (PEST) and 500 μg/mL Geneticin/G418. HEK293-cells stably transfected with human CCR1 and CCR2 were cultured in Dulbecco's Modified Eagle Medium (DMEM) containing pyruvate and Glutamax and supplemented with 10% FBS (from PAA, Austria), 100 U/ml penicillin, and 100 μg/mL streptomycin (PEST). Selection was performed with 330 μg/mL Geneticin. Cells were harvested at 60% confluence in buffer containing 10 mM Tris-HCl pH 7.4, 5 mM EDTA, and 0.1 mg/mL bacitracin and centrifuged at 100*g* for for 10 min (4 °C). The cell pellet was resuspended in harvesting buffer, pooled, and homogenized using a Dounce homogenizer. The homogenate was centrifuged in 48000*g* for 10 min. (4 °C) and resuspended in harvesting buffer using Ultra-Turrax T8. Membrane aliquots were stored at −80 °C. Protein concentration was determined using a modified method by Lowry.[32]

Binding Studies Using [^{125}I]CX$_3$CL1. Saturation binding studies were carried out in duplicates in polypropylene tubes in a total volume of 1 mL of binding buffer containing 50 mM HEPES, 10 mM $MgCl_2$, 1 mM EDTA, and 0.1% gelatin (pH 7.4) and 0.05−150 pM [^{125}I]CX$_3$CL1 (8−12 concentrations). Nonspecific binding was determined in the presence of 10 nM unlabeled CX$_3$CL1. The reaction was started by the addition of 1 μg/tube of hCX$_3$CR1/Gαqi5 membranes and incubated for 24 h in room temperature. The reaction was terminated by rapid filtration through Whatman GF/B filters (pretreated with 0.3% polyethyleneimine, PEI) followed by subsequent washing with cold washing buffer (10 mM Hepes, 500 mM NaCl, pH 7.4 at 4 °C) using a Brandel cell harvester. Scintillation cocktail (Packard Ultima Gold, 4 mL) was added and the radioactivity determined in a scintillation counter (Packard 2900TR liquid scintillation counter). Competition studies were performed with [^{125}I]CX$_3$CL1 (15−37 pM) in the presence of increasing concentration of test compound diluted in DMSO (final concentration of 1%) and 1.5 pM hCX$_3$CR1 receptors per tube in a total volume of 1 mL binding buffer. The competition binding experiments were run for 24 h in room temperature and terminated as described for the saturation binding studies. The K_i values (inhibition constants) of the test compounds were calculated from the observed IC_{50} of the test compound using the Cheng−Prusoff equation. The K_d value for [^{125}I]CX$_3$CL1 used for calculation of K_i were determined as described above for saturation binding studies, and were 9.55 pM (pK_d 11.02 ± 0.05, n = 3)

Competition Binding with CXCR2, CCR1, and CCR2 Receptors. Radioligands [^{125}I]-humanIL8 ([^{125}I]-hIL8), [^{125}I]MIP-1α, and [^{125}I]MCP-1 are used to study the CXCR2, CCR1, and CCR2 receptors, respectively. The CXCR2 competition binding assay was performed in white clear bottom 96-well isoplates in a total volume of 200 μL/well. Each well contained 150 pM [^{125}I]-hIL8, membrane preparation equivalent to a receptor concentration of 20 pM, 1.5 mg of WGA SPA-beads in assay buffer [50 mM HEPES-KOH pH 7.4, 10 mM $MgCl_2$, 1 mM EDTA, 0.5% (w/v) gelatin], and increasing concentrations of test compounds diluted in DMSO (final concentration of 1% (v/v)). The nonspecific binding (min binding) was defined by 500 nM unlabeled hIL8. The assay was incubated at room temperature for 4 h, and then the assay plates were counted in Microbeta Trilux 1450. The CCR1 and CCR2 competition binding assays were performed in 2 mL deep well plates in a total volume of 1 mL. Each well contained 15−20 pM [^{125}I]MIP-1α or [^{125}I]MCP-1, 2 pM hCCR1, or 1.5 pM CCR2 receptors in assay buffer (50 mM Hepes, 10 mM $MgCl_2$, 1 mM EDTA, 0.1% gelatin, pH 7.4) and increasing concentrations of test compounds diluted in DMSO (final concentration of 1% (v/v). Nonspecific binding was defined with 10 nM unlabeled peptide. The assays were incubated at room temperature for 24 h and terminated by rapid filtration through Whatman GF/B filters pretreated with 0.3% PEI, followed by subsequent washing with cold buffer (10 mM Hepes, 500 mM NaCl, pH 7.4 at 4 °C) using a TomTec harvester. Meltilex melt-on scintillator was added and the radioactivity determined in a scintillation counter (Wallac 1205 Betaplate). The K_i values (inhibition constants) of the test compounds were calculated from the observed IC_{50} of the test compound using the Cheng−Prusoff equation. The K_d values used in the calculation of the K_i values were determined in saturation binding experiments under the corresponding competition assay conditions, and were 93, 13, and 19 pM for CXCR2, CCR1, and CCR2 respectively.

Solubility Assay. The HT (high throughput) solubility screening protocol[33] used a 10 mM DMSO stock solution of the compound and was performed in a 96-well format. A concentration of 100 μM (1% DMSO) was incubated in 0.1 M phosphate buffer, pH 7.4, for 24 h under gentle shaking (<500 rpm) on a plate bed shaker at room temperature in duplicate (2 μL till 200 μL applied in a Costar PP 96-well plate, 350 μL). The solution was filtered from undissolved material (Multiscreen-R4, 0.4 μm Hydrophilic PTFE LCR Membrane, Glass-Filled PP filtration plate, Millipore AB) prior to LC-UV-DAD-MS analysis. UV quantification was performed at the most sensitive wavelength chosen from the DAD spectrum relative to two standard solutions, 10 μM and 100 μM in DMSO, with a detection limit of 0.01 μM. If the solubility was found to be >100 μM, it is reported as "100 μM". Estimated variation of solubility rank value: ±10−20%.

Analysis. The physical chemical properties (identity, purity, stability, and solubility) were run simultaneously using a generic LC-UV-DAD-MS method (Waters 2790 Alliance HPLC-996 DAD-ZQ MS system). The chromatographic separation was performed on RP narrow bore columns, XTerra MS C18 2.1 mm × 100 mm, 3.5 m or equivalent, with a fast HPLC gradient in a formic acid/acetonitrile system (5−100%) at a flow rate of 0.3 mL/min. Mass spectrometry was performed with electrospray ionization under generic conditions with confirmation of the molecular weight with full scan acquisition in positive and negative ion mode. The sample preparation was performed from 10 mM in DMSO or using solid material. The DMSO stock solutions as well as diluted solutions were checked for precipitation. For each sample or standard, an injection of 20 μL was made.

Permeability Assay. Permeability in Caco-2 cells was measured in the A−B direction at pH 6.5.[34] Permeability experiments were carried out in Hank's Buffered Salt Solution buffered supplemented with 25 mM MES at pH 6.5 (buffer A) and Hank's Buffered Salt Solution buffered supplemented with 25 mM HEPES at pH 7.4 (buffer B). Compounds were dissolved in DMSO and diluted to 10 μM in buffer A. Three inserts with cells and one without were used for each experiment. The experiments were carried out on filter-grown cell monolayers that were equilibrated in transport buffer at 37 °C for 10 min in a shaking incubator. The basolateral wells contained 0.80 mL of buffer B, and the apical wells contained 0.20 mL of buffer A. After removal of buffer from both sides, the test compound in buffer A was added to the donor side and fresh buffer B was added to the receiver side. The experiments were carried out in a humidified atmosphere of CO_2/air (5%/95%) at 37 °C for 90 min. Samples were taken from the donor side in the beginning and at the end (90 min.) of the experiment, and samples were taken from the receiver side at 45 and 90 min. Equal volume of fresh buffer was replenished. The integrity of the epithelial cell monolayer was monitored by measurements of passive transmembrane diffusion of radiolabeled [^{14}C]mannitol. Concentrations of the compound in both donor and receiver samples were analyzed by LC-MS. Liquid scintillation was used for analysis of [^{14}C]mannitol. Data is presented as means of triplicate measuments. Mass balances calculations were based on total recovery of parent molecule at the end of the experiment. All incubations contained less than 1% total DMSO.

Metabolic Stability Assay. Metabolic stability was measured in human microsomes. Microsome incubations for Cl_{int} (intrinsic

Table 8. Gradient Details for LC methods A, B, and C

LC gradient method A			LC gradient method B			LC gradient method C		
time (min)	vol % A	vol % B	time (min)	vol % A	vol % B	time (min)	vol % A	vol % B
0	100	0	0	100	0	0	100	0
0.1	65	35	0.1	70	30	0.1	65	35
18	65	35	11	65	35	11	60	40
18.8	0	100	12	0	100	12	0	100
19.5	0	100	12.8	0	100	12.8	0	100
19.8	100	0	13	100	0	13	100	0

clearance) determinations and metabolic profiling experiments were conducted as previously described.[35] Briefly, microsomes at the concentration 0.5 mg protein/mL supplemented with 1 mM NADPH were incubated at 37 °C with gentle shaking in a 5% CO2 atm. All incubations were stopped by the addition of two volumes of ice-cold acetonitrile and were then centrifuged prior to LC-MS/MS analysis. The metabolic capacity of the microsomes was checked in-house using a set of probe substrates. Cl_{int} values were obtained from disappearance curves of the parent molecule.[36] LC-MS analysis for Cl_{int} value estimations was performed with a Micromass Quattro Micro triple quandropole as previously described.[36]

In Vivo Pharmacokinetic Assay. In vivo pharmaocokinetics in rat was assessed in male Sprague−Dawley rats:[37] Male Sprague−Dawley rats (Scanbur B&K AB, Sollentuna, Sweden) were housed with up to five animals per cage and were allowed to acclimatize to the new environment for at least one week upon arrival. In the conditioned animal facility, room temperature was kept at 20 ± 2 °C, relative humidity at 60 ± 20%, and a 12 h light−dark cycle was maintained including a 0.5 h dusk or dawn period (lights on at 6.30 a.m.). Water and standard rodent diet (R70 Lactamin, Stockholm, Sweden) were freely accessible. All animal handling and experiments were performed in full compliance with authorial and ethical guidelines (Ethical Board of South Stockholm). Diet was removed from the animals 1 h prior to dose administration and replaced 6 h after dose administration. Rats (∼300 g) were weighed and divided into two groups: one group (n = 3) received 3 μmol/kg of the test compound intravenously (iv) as a bolus injection in the tail vein, the other group received 10 μmol/kg orally (po) via gavage in a parallel study design. All compounds were given discretely. The dose volume was 4 mL/kg for both dose routes. All compounds were formulated in 5% dimethylamine, 20% hydroxypropyl-β-cyclodextrine in 0.1 M Meglumin for both iv and po adminstration. For each dose occasion a fresh formulation was prepared. To verify the concentration of the administered dose, an aliquot of each formulation was taken, transferred to a polypropylene tube (Cryotubes, A/S Nunc, Denmark) and diluted 10 times with MeCN before analysis. Blood samples (400 μL) from the tail vein were collected in microtainer tubes (BD, Plymouth, UK) containing EDTA at 0.02, 0.08, 0.33, 0.67, 1, 3, 6, and 24 h following iv administration, or at 0.25, 0.5, 0.75, 1, 1.5, 2.5, 6, and 24 h following po administration. The blood samples were centrifuged for 5 min at 2000g (4 °C). The supernatant was transferred to polypropylene tubes and stored at −20 °C until analysis. Polypropylene tubes (1.5 mL per tube) in 96-well format used for storage of plasma samples were obtained from Biotech Solutions (Vineland, NJ, USA). The samples were then analyzed by LC-MS as previously described.[37,38]

Chemistry. *General Experimental Section.* Starting materials used were either available from commercial sources or prepared according to literature procedures. Reactions were typically run under an inert atmosphere of nitrogen or argon in commercially available anhydrous solvents that were used without further purification or drying. Room temperature refers to 20−25 °C. Final compounds were purified to >95% purity as determined by HPLC analysis.

Microwave heating was performed in a Creator or Smith Synthesizer single mode microwave cavity producing continuous irradiation at 2450 MHz at the indicated temperature in the recommended microwave tubes.

The ^{1}H and ^{13}C NMR spectra were recorded at room temperature unless otherwise stated, using an NMR spectrometer (Bruker or Varian) fitted with a probe of suitable configuration. ^{1}H NMR spectra were recorded at 400, 500, or 600 MHz. ^{13}C NMR spectra were recorded at 100 or 126 MHz. Chemical shifts are given in ppm down- and upfield from TMS (0.00 ppm). The following reference signals were used: TMS δ 0.00, or the residual solvent signal of DMSO-d_6 δ 2.50 (^{1}H), δ 39.51 (^{13}C), CD_3OD δ 3.30 (^{1}H), δ 49.00 (^{13}C), $CDCl_3$ δ 7.26 (^{1}H), δ 77.16 (^{13}C), CD_3CN δ 1.94 (^{1}H), δ 118.26 (^{13}C), or TFA δ 11.50 (^{1}H), δ 164.2 (^{13}C) (unless otherwise indicated). Resonance multiplicities are denoted s, d, t, q, m, br, and app for singlet, doublet, triplet, quartet, multiplet, broad, and apparent, respectively.

The mass spectra were typically recorded utilizing thermospray (Finnigan MAT SSQ 7000; buffer, 50 nM NH_4OAc in CH_3CN:H_2O; 3:7), electron impact (Finnigan MAT SSQ 710), or electrospray (LC-MS; LC, Waters 2790, column XTerra MS C8 2.5 μm 2.1 mm × 30 mm, buffer gradient H_2O + 0.1%TFA:CH_3CN + 0.04%TFA; MS, micromass ZMD) ionization techniques.

Preparative HPLC was run on a Waters autopurifier HPLC with a diode array detector. Column: Xterra MS C8, 19 mm × 300 mm, 10 μm. Narrow gradients with MeCN/water were used at a flow rate of 20 mL/min.

Thin layer chromatography (TLC) was performed on Merck TLC-plates (Silica gel 60 F254) and UV visualized the spots.

Column chromatography was performed using Merck Silica gel 60 (0.040−0.063 mm).

GC-analyses were performed on a GC 6890 (Agilent technologies) equipped with a flame ionization detector. The column used for analysis of enantiomeric purity was a Cyclodex B (ID 0.25 mm × 30 m, 0.25 μm, Agilent technologies) using the specified temperature program.

Analytical separation of diastereoisomers of compounds **18** and **24**: LC-MS analyses were performed on an LC-MS system consisting of a Waters Alliance 2795 HPLC, a Waters PDA 2996 diode array detector, and a ZQ 2000 single quadrupole mass spectrometer. The mass spectrometer was equipped with an electrospray ion source (ES) operated in positive and negative ion mode. The capillary voltage was set to 3.0 V and the cone voltage to 30 V. The mass spectrometer was scanned between m/z 160−600 with a scan time of 0.5 s. The diode array detector scanned from 210 to 350 nm. The column oven temperature was set to 40 °C Separation was performed on a Waters XTerraMS, C8, 3.5 μm, 2.1 mm × 50 mm. Mobile phase A: formic acid (10.6 mM) in water/acetonitrile (95:5). Mobile phase B: formic acid (10.6 mM) in water/acetonitrile (2:98). For each structure a special separation LC gradient was developed, details on the gradients are given Table 8 for LC methods A, B, and C.

Representative experimental procedures for the synthesis of compounds discussed in this publication are presented below; further experimental details and analytical data can be found in the Supporting Information.

*4-Amino-2-(benzylsulfanyl)-6-oxo-1,6-dihydropyrimidin-5-yl thiocyanate (**7**).* 6-Amino-2-(benzylsulfanyl)pyrimidin-4-ol[38] (**6**) (70 g, 300.1 mmol) and KSCN (120 g, 1.23 mol) were suspended in DMF (1.5 L) and heated to 65 °C. Pyridine (40.4 g, 510 mmol) was added, and the solution was cooled to 5 °C. Bromine (43.2 g, 270 mmol) was added dropwise, and the solution was stirred for 2 h at 5−10 °C and then overnight at room temperature. The mixture was poured into ice water and stirred for 1 h. The solid product was collected by filtration, washed with cold water, and then dried in vacuo. The procedure was repeated once more starting from 67 g of 6-amino-2-(benzylsulfanyl)-

dx.doi.org/10.1021/jm3012273 | J. Med. Chem. 2013, 56, 3177−3190

pyrimidin-4-ol. The combined batches of the title compound (170.5 g) was used directly in the next step without further purification. ^{1}H NMR (400 MHz, DMSO-d_6) δ ppm 12.34 (br s, 1H), 8.00−7.50 (br s, 2H), 7.46 (d, J = 7.6 Hz, 2H), 7.39−7.21 (m, 3H), 4.38 (s, 2H). ^{13}C NMR (101 MHz, DMSO-d_6) δ ppm 163.5, 162.7, 160.7, 137.2, 129.2, 128.4, 127.4, 111.9, 72.8, 33.5.

*2-Amino-5-(benzylsulfanyl)[1,3]thiazolo[4,5-d]pyrimidin-7-ol (**8**).* 4-Amino-2-(benzylsulfanyl)-6-oxo-1,6-dihydropyrimidin-5-yl thiocyanate (**7**) (170.5 g, 587 mmol) was suspended in water (0.33 L) and DMF (1 L) and heated at 120 °C for 27 h. The reaction mixture was poured onto ice, and the resulting pale-yellow precipitate was collected by filtration and washed with water. The solid material was suspended in water (2.5 L) and heated to 75 °C, and sodium hydroxide (10 M solution in water, 170 mL) was added. The resulting slightly cloudy suspension was filtered, and the product was precipitated by addition of concd HCl until pH 4. The solids were collected by filtration and dried in vacuo over P_2O_5. Excess water was coevaporated with acetonitrile, and the resulting material was dried in vacuo overnight to give the title compound (170 g, 100% yield, 98% purity). ^{1}H NMR (400 MHz, DMSO-d_6) δ ppm 12.53 (br s, 1H), 8.17 (s, 2H), 7.43 (d, d, J = 7.1 Hz, 2H), 7.20−7.35 (m, 3H), 4.41 (s, 2H). ^{13}C NMR (101 MHz, DMSO-d_6) δ ppm 171.9, 168.4, 157.2, 137.4, 129.2, 129.1, 128.4, 127.3, 103.0, 33.7. MS (ES+) m/z 291.0 $[M + H]^+$.

*5-(Benzylsulfanyl)-7-chloro[1,3]thiazolo[4,5-d]pyrimidin-2-amine (**9**).* 2-Amino-5-(benzylsulfanyl)[1,3]thiazolo[4,5-d]pyrimidin-7-ol (**8**) (8.0 g, 27.6 mmol) was suspended in $POCl_3$ (80 mL), and *N,N*-dimethylaniline (8 mL) was added. The mixture was heated at reflux for 3 h. After cooling to room temperature, the reaction mixture was slowly added to a stirred mixture of ice and water. The resulting precipitate was collected by filtration. The solid material was purified by silica gel column chromatography using 30−50% EtOAc in $CHCl_3$ to give the title compound as a yellow solid (5.11 g, 60% yield, 95% purity). ^{1}H NMR (400 MHz, DMSO-d_6) δ ppm 8.96 (br s, 2H), 7.40−7.47 (m, 2H), 7.19−7.34 (m, 3H), 4.37 (s, 2H). ^{13}C NMR (101 MHz, DMSO-d_6) δ ppm 172.8, 170.9, 167.4, 148.9, 137.7, 129.0, 128.4, 127.1, 117.6, 34.5. MS (ES+) m/z 309.0 $[M + H]^+$.

*General Method **1**.* Synthesis of 5-(benzylsulfanyl)[1,3]thiazolo-[4,5-d]pyrimidin-2-amine aminoalcohol derivatives **11**.

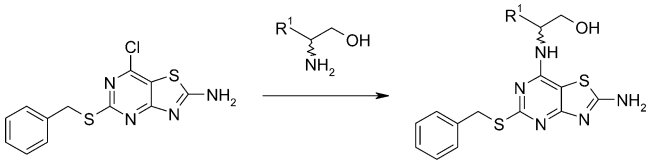

To an approximately 0.05−0.6 M solution of 5-(benzylsulfanyl)-7-chloro[1,3]thiazolo[4,5-d]pyrimidin-2-amine (**9**) (1.0 equiv) in anhydrous *N*-methylpyrrolidone were added an aminoalcohol (**10**) (1.4−4.0 equiv) and *N,N*-diisopropylethylamine (1.1−4.0 equiv). The reaction mixture was stirred and heated at 100−130 °C (oil bath temperature) for 18−96 h or heated in a microwave oven at 120−200 °C for 5 min−1 h. The mixture was poured into an ice/water slurry, stirred until the ice was melted, and then it was filtered. The resulting precipitate was purified for example by coevaporation with toluene/ethanol, purification by silica gel column chromatography, recrystallization in dichloromethane, or washing with water, followed by an organic solvent and dried in vacuo over P_2O_5 to give the 5-benzylsulfanyl)[1,3]thiazolo[4,5-d]pyrimidin-2-amine aminoalcohol derivatives **11a−f**.

*(2R)-2-[(2-Amino-5-sulfanyl[1,3]thiazolo[4,5-d]pyrimidin-7-yl)-amino]-4-methylpentan-1-ol (**12a**).* Liquid ammonia (500 mL) was condensed into a 1 L flask (dry ice/acetone cooling bath) and (2*R*)-2-{[2-amino-5-(benzylsulfanyl)[1,3]thiazolo[4,5-d]pyrimidin-7-yl]-amino}-4-methylpentan-1-ol (**11a**) (13.0 g, 33.4 mmol) was carefully added under a N_2-atmosphere. To the clear solution was added an excess of sodium metal in small pieces, until a blue color persisted. When the blue color had remained for 25 s, solid ammonium chloride was added to quench the reaction. The ammonia was removed under a stream of N_2, and the remains were dissolved in water (300 mL). The mixture was filtered, and the resulting clear solution was neutralized (pH 7) with concd HCl. The precipitated solid was collected by filtration, washed with water and acetonitrile, and dried at 50 °C in vacuo for 2 h and over P_2O_5 overnight in vacuo to give the title compound (8.57 g, 86% yield) as a yellow solid. ^{1}H NMR (400 MHz, DMSO-d_6) δ ppm 12.74 (s, 1H), 8.44 (br s, 2H), 7.41 (d, J = 8.59 Hz, 1H), 4.75−4.87 (m, 1H), 4.31−4.43 (m, 1H), 3.37−3.46 (m, 2H, overlapping with the water signal), 1.51−1.65 (m, 1H), 1.33−1.47 (m, 2H), 0.82−0.94 (m, 6H). ^{13}C NMR (101 MHz, DMSO-d_6) δ ppm 177.1, 172.6, 158.1, 155.9, 154.1, 92.1, 63.7, 50.2, 24.4, 23.4, 22.0. MS (ES+) m/z 300 $[M + H]^+$.

*General Method **2**.* Synthesis of compounds **14** and **18**.

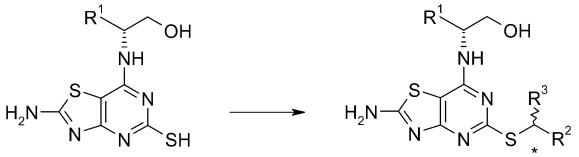

(2*R*)-2-[(2-Amino-5-sulfanyl[1,3]thiazolo[4,5-d]pyrimidin-7-yl)-amino]-4-methylpentan-1-ol (**12a**) (30 mg, 100 μmol) was suspended in DMSO (450 μL). Optionally, sodium borohydride (0.1−1 equiv) was added. Diisopropylethylamine (19 μL, 110 μmol) was added, followed by the quick addition of the organic halide (**13** or **17**) (105 μmol). The reaction was stirred for 1−20 h at room temperature or 40 °C. The mixture was poured onto ice, and the solid product was collected by filtration after the ice had melted and then washed with water to give the title compound after drying in vacuo. Alternatively, the crude product was purified by reverse phase preparative HPLC or silica gel chromatograpy to give the title compound **14** or **18**.

*(2R)-2-{[5-(Benzylsulfanyl)-2-chloro[1,3]thiazolo[4,5-d]pyrimidin-7-yl]amino}-4-methylpentan-1-ol (**19a**).* The reaction was split into two separate 2 L round-bottomed flasks, and the two reaction mixtures were pooled before work up. To a solution of (2*R*)-2-{[2-amino-5-(benzylsulfanyl)[1,3]thiazolo[4,5-d]pyrimidin-7-yl]amino}-4-methylpentan-1-ol (**11a**) (42.0 g, 10.8 mmol) in acetonitrile (1.1 L) and 37% hydrochloric acid (1.5 L) was added sodium nitrite (14.9 g, 21.6 mmol, dissolved in a small amount of water) dropwise. The mixture was kept on ice during the addition to keep the temperature <5 °C and was then stirred at 0 °C for 5 h. The reaction flask was kept in the refrigerator overnight and was thereafter stirred at 5 °C until completion (27 h in total). The reaction mixture was filtered. The filtrate was poured onto ice. The mixture was filtered after the ice had melted and the collected solid was washed with water. Acetonitrile was added, and the solvent was evaporated. The product was dried at 50 °C in vacuo to give the title compound (34.7 g, 79% yield) as a pink solid. The product was used as such in the next step. MS (ES+) m/z 409 $[M + H]^+$.

*(2R)-2-{[5-(Benzylsulfanyl)-2-methoxy[1,3]thiazolo[4,5-d]-pyrimidin-7-yl]amino}-4-methylpentan-1-ol (**20a**).* To a solution of (2*R*)-2-{[5-(benzylsulfanyl)-2-chloro[1,3]thiazolo[4,5-d]pyrimidin-7-yl]amino}-4-methylpentan-1-ol (**19a**) (34.7 g, 84.8 mmol) in methanol (870 mL) was added potassium hydroxide (9.5 g, 170 mmol), and the mixture was heated at 55 °C for 20 min. The solvent was evaporated. Dichloromethane (350 mL) and water (350 mL) were added, resulting in a thick slurry. The organic solvent was evaporated, and the aqueous mixture was filtered. The solid was collected and recrystallized in acetonitrile (350 mL) and dried at 40 °C in vacuo for 4 h to give the title compound (26.5 g, 77% yield) as a pale-orange solid. ^{1}H NMR (500 MHz, DMSO-d_6) δ ppm 7.54 (d, J = 8.51 Hz, 1H), 7.42 (d, J = 7.25 Hz, 2H), 7.30 (t, J = 7.57 Hz, 2H), 7.21−7.26 (m, 1H), 4.74 (t, J = 4.73 Hz, 1H), 4.26−4.41 (m, 3H), 4.16 (s, 3H), 3.35−3.46 (m, 2H, overlapping with the water signal), 1.53−1.65 (m, 1H), 1.35−1.49 (m, 2H), 0.87 (d, J = 6.62 Hz, 3H), 0.83 (d, J = 6.62 Hz, 3H). ^{13}C NMR (126 MHz, DMSO-d_6) δ ppm 177.5, 166.8, 164.7, 156.1, 138.3, 128.6, 128.2, 126.7, 100.3, 63.3, 59.4, 50.3, 34.0, 24.2, 23.2, 21.8. MS (ES+) m/z 405 $[M + H]^+$.

*5-(Benzylsulfanyl)-7-{[(2R)-1-hydroxy-4-methylpentan-2-yl]-amino}[1,3]thiazolo[4,5-d]pyrimidin-2(3H)-one (**21a**).* To a solution of (2*R*)-2-{[5-(benzylsulfanyl)-2-methoxy[1,3]thiazolo[4,5-d]-

dx.doi.org/10.1021/jm3012273 | J. Med. Chem. 2013, 56, 3177−3190

pyrimidin-7-yl]amino}-4-methylpentan-1-ol (**20a**) (26.5 g, 65.4 mmol) in 1,4-dioxane (790 mL) and water (16 mL) 37% hydrochloric acid (14 mL) was added, and the mixture was heated at 45 °C for 18 h. The solvent was evaporated, and the crude product was crystallized from ethyl acetate/dichloromethane, 3:7 resulting in crop 1. The mother liquid was concentrated, and the residue was crystallized from ethyl acetate/tetrahydrofuran resulting in crop 2. The mother liquid was once again concentrated, and the residue was added to a silica gel column and was eluted with 30% ethyl acetate in dichloromethane, resulting in crop 3. The crops were pooled, tetrahydrofuran was added, and the solvent was evaporated. The product was dried at 40 °C in vacuo for 5 h to give the title compound (13.6 g, 53% yield) as a pink solid. ^{1}H NMR (500 MHz, DMSO-d_6) δ ppm 12.38 (br s, 1H), 7.42 (d, J = 7.57 Hz, 2H), 7.20−7.31 (m, 4H), 4.25−4.37 (m, 3H), 3.30−3.44 (m, 2H), 1.53−1.63 (m, 1H), 1.32−1.47 (m, 2H), 0.86 (d, J = 6.62 Hz, 3H), 0.82 (d, J = 6.62 Hz, 3H). ^{13}C NMR (126 MHz, DMSO-d_6) δ ppm 169.4, 166.7, 155.0, 154.4, 138.6, 129.0, 128.5, 127.1, 91.0, 63.7, 50.6, 34.2, 24.5, 23.5, 22.1. MS (ES+) m/z 391 $[M + H]^+$.

General Method ***3***. Synthesis of compound **22**.

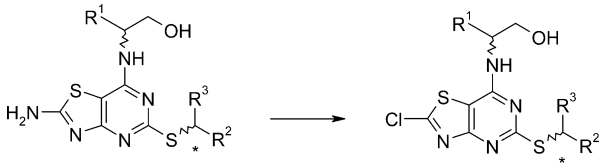

Concd HCl (2.5 mL/mmol of a compound **18**) was added to compound **18** (1.0 equiv) in CH_3CN. The reaction mixture was cooled in an ice bath, and sodium nitrite (2.0 equiv) dissolved in a minimal amount of water was added dropwise. The reaction was stirred at 0 °C until the reaction was complete (monitored by LC-MS, HPLC, or TLC) and was then poured into ice water, neutralized with sodium bicarbonate, and extracted with DCM or EtOAc. The combined organic phases were dried and concentrated in vacuo to give product compound **22**.

General Method ***4***. Synthesis of compound **23**.

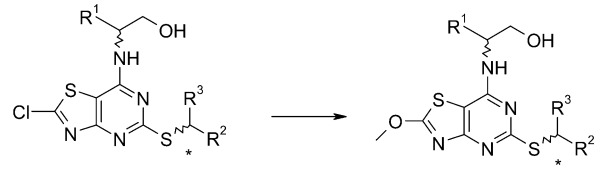

Potassium hydroxide (2.0 equiv) dissolved in methanol was added dropwise to a cooled (0 °C) solution of compound **22** (1.0 equiv) in methanol. The resulting mixture was stirred at 0 °C until the reaction was complete (monitored by LC-MS, HPLC, or TLC). The solvent was evaporated and the product **23** was used in the next reaction step without further purification.

General Method ***5***. Synthesis of compound **24**.

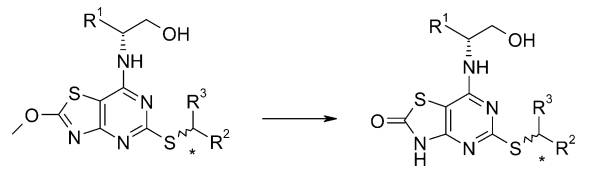

A solution of concentrated HCl (1.0 equiv) was added to a cooled (0 °C) solution of compound **23** (1.0 equiv) in 1,4-dioxane. The resulting mixture was stirred at 40 °C until the reaction was complete (monitored by LC-MS, HPLC, or TLC). The reaction mixture was neutralized with saturated $NaHCO_3$ (aq), and the dioxane was evaporated. The residue was dissolved in DCM or EtOAc, washed with brine, dried, and concentrated in vacuo. The crude product **24** was, if necessary, purified using preparative HPLC or by flash silica gel column chromatography.

■ ASSOCIATED CONTENT

Ⓢ Supporting Information

Experimental procedures and experimental data for intermediates and final compounds not present in the Experimental Section. This material is available free of charge via the Internet at http://pubs.acs.org.

■ AUTHOR INFORMATION

Corresponding Author

*For S. K.: phone, +46-(0)70-3355543; E-mail, Sofia.Karlstrom@medivir.com. For R. J.: phone, +46-(0)-73-3542157; E-mail, daggstigen@gmail.com.

Present Address

The research unit where this work was conducted, AstraZeneca Research and Development, Södertälje, Sweden, was closed in 2012. Contact with the authors can be made using the information below. For S.K.: Medivir AB, P.O. Box 1086, SE-141 22 Huddinge, Sweden. For R.J.: Daggstigen 8B, SE-141 38 Huddinge, Sweden. For G.N.: AlzeCure Discovery, NVS Huddinge Hospital, Novum lv 5, SE-141 57 Huddinge, Sweden. For P.H.S.: Department of Applied Physical Chemistry, Royal Institute of Technology, SE-10044 Stockholm, Sweden and SP Process Development, SE-151 21 Södertälje, Sweden.

Author Contributions

The manuscript was written through contributions of all authors. All authors have given approval to the final version of the manuscript. S.K., G.N., and R.J. contributed equally.

Notes

The authors declare no competing financial interest.

■ ACKNOWLEDGMENTS

We thank Margareta Bergh and the Physiochemical Characterization Team at the Department of Medicinal Chemistry at AstraZeneca Södertälje for physiochemical characterization including solubility measurements, and the Analytical & Purification Sciences Team for separations, purifications, and NMR analyses of compounds. We also acknowledge Sanna Laine and Eva Blomberg for in vitro characterizations of the compounds.

■ ABBREVIATIONS USED

ADAM, a disintegrin and metalloproteinase domain-containing protein; CCL, CC chemokine ligand; CCR, CC chemokine receptor; CD, cluster of differentiation; Cl_{int}, intrinsic clearance; CXCR, CXC chemokine receptor; CX_3CL1, chemokine (C-X3-C motif) ligand 1; CX_3CR1, CX_3C chemokine receptor 1, fractalkine receptor; DIPCl, B-chlorodiisopinocampheylborane; FKN, fractalkine; hERG, the human ether-à-go-go-related gene; HT, high throughput; HTS, high throughput screening; NCS, *N*-chlorosuccinimide; NK-cell, natural killer cell; Papp, apparent permeability coefficient; TACE, tumor necrosis factor-α-converting enzyme

■ REFERENCES

(1) (a) Pan, Y.; Lloyd, C.; Zhou, H.; Dolich, S.; Deeds, J.; Gonzalo, J.-A.; Vath, J.; Gosselin, M.; Ma, J.; Dussault, B.; Woolf, E.; Alperin, G.; Culpepper, J.; Gutierrez-Ramos, J. C.; Gearing, D. Neurotactin, a membrane-anchored chemokine upregulated in brain inflammation. *Nature* **1997**, *387*, 611−617. (b) Bazan, J. F.; Bacon, K. B.; Hardiman, G.; Wang, W.; Soo, K.; Rossi, D.; Greaves, D. R.; Zlotnik, A.; Schall, T. J. A new class of membrane-bound chemokine with a CX_3C motif.

Nature **1997**, *385*, 640−644. (c) Imai, T.; Hieshima, K.; Haskell, C.; Baba, M.; Nagira, M.; Nishimura, M.; Kakizaki, M.; Takagi, S.; Nomiyama, H.; Schall, T. J.; Yoshie, O. Identification and molecular characterization of fractalkine receptor CX_3CR1, which mediates both leukocyte migration and adhesion. *Cell* **1997**, *91*, 521−530.

(2) Hundhausen, C.; Misztela, D.; Berkhout, T. A.; Broadway, N.; Saftig, P.; Reiss, K.; Hartmann, D.; Fahrenholz, F.; Postina, R.; Metthews, V.; Kallen, K.-J.; Rose-John, S.; Ludwig, A. The disintegrin-like metalloproteinase ADAM10 is involved in constitutive cleavage of CX_3CL1 (fractalkine) and regulates CX_3CL1-mediated cell−cell adhesion. *Blood* **2003**, *102*, 1186−1195.

(3) Wiener, J. J. M.; Sun, S.; Thurmond, R. L. Recent advances in the design of cathepsin S inhibitors. *Curr. Top. Med. Chem.* **2010**, *10*, 717−732.

(4) Raport, C. J.; Schweickart, V. L.; Eddy, R. L., Jr.; Shows, T. B.; Gray, P. W. The orphan G-protein-coupled receptor-encoding gene V28 is closely related to genes for chemokine receptors and is expressed in lymphoid and neural tissues. *Gene* **1995**, *163*, 295−299.

(5) Harrison, J. K.; Jiang, Y.; Chen, S.; Xia, Y.; Maciejewski, D.; McNamara, R. K.; Streit, W. J.; Salafranca, M. N.; Adhikari, S.; Thompson, D. A.; Botti, P.; Bacon, K. B.; Feng, L. Role for neuronally derived fractalkine in mediating interactions between neurons and CX3CR1-expressing microglia. *Proc. Natl. Acad. Sci. U. S. A.* **1998**, *95*, 10896−10901.

(6) Nishimura, M.; Umehara, H.; Nakayama, T.; Yoneda, O.; Hieshima, K.; Kakizaki, M.; Dohmae, N.; Yoshie, O.; Imai, T. Dual functions of fractalkine/CX3C ligand 1 in trafficking of perforin +/granzyme B+ cytotoxic effector lymphocytes that are defined by CX3CR1 expression. *J. Immunol.* **2002**, *168*, 6173−6180.

(7) Ancuta, P.; Liu, K.-Y.; Misra, V.; Acleche, V. S.; Gosselin, A.; Zhou, X.; Gabuzda, D. Transcriptional profiling reveals developmental relationship and distinct biological functions of CD16+ and CD16- monocyte subsets. *BMC Genomics* **2009**, *10*, 403−421.

(8) Tacke, F.; Randolph, G. J. Migratory fate and differentiation of blood monocyte subsets. *Immunobiology* **2006**, *211*, 609−618.

(9) Ziegler-Heitbrock, L. The CD14+ CD16+ blood monocytes: their role in infection and inflammation. *J. Leukocyte Biol.* **2007**, *81*, 584−592.

(10) Fingerle-Rowson, G.; Angstwurm, M.; Andreesen, R.; Ziegler-Heitbrock, H. L. W. Selective depletion of CD14+ CD16+ monocytes by glucocorticoid therapy. *Clin. Exp. Immunol.* **1998**, *112*, 501−506.

(11) Hanai, H.; Iida, T.; Takeuchi, K.; Watanabe, F.; Yamada, M.; Kikuyama, M.; Maruyama, Y.; Iwaoka, Y.; Hirayama, K.; Nagata, S.; Takai, K. Adsorptive depletion of elevated proinflammatory CD14+CD16+DR++ monocytes in patients with inflammatory bowel disease. *Am. J. Gastroenterol.* **2008**, *103*, 1210−1216.

(12) Gevrey, J.-C.; Isaac, B. M.; Cox, D. Syk Is Required for Monocyte/Macrophage Chemotaxis to CX3CL1 (Fractalkine). *J. Immunol.* **2005**, *175*, 3737−3745.

(13) Schulz, C.; Schäfer, A.; Stolla, M.; Kerstan, S.; Lorenz, M.; von Brühl, M.-L.; Schiermann, M.; Bauersachs, J.; Gloe, T.; Busch, D. H.; Gawaz, M.; Massberg, S. Chemokine fractalkine mediates leukocyte recruitment to inflammatory endothelial cells in flowing whole blood: a critical role for P-selectin expressed on activated platelets. *Circulation* **2007**, *116*, 764−773.

(14) Man, S.; Ubogu, E. E.; Ranshoff, R. M. Inflammatory cell migration into the central nervous system: a few new twists on an old tale. *Brain Pathol.* **2007**, *17*, 243−250.

(15) Haskell, C. A.; Cleary, M. D.; Charo, I. F. Molecular uncoupling of fractalkine-mediated cell adhesion and signal transduction. Rapid flow arrest of CX_3CR1-expressing cells is independent of G-protein activation. *J. Biol. Chem.* **1999**, *274*, 10053−10058.

(16) Mizoue, L. S.; Bazan, J. F.; Johnson, E. C.; Handel, T. M. Solution Structure and Dynamics of the CX_3C Chemokine Domain of Fractalkine and Its Interaction with an N-Terminal Fragment of CX_3CR1. *Biochemistry* **1999**, *38*, 1402−1414.

(17) (a) Onuffer, J. J.; Horuk, R. Chemokines, chemokine receptors and small-molecule antagonists: recent developments. *Trends Pharmacol. Sci.* **2002**, *23*, 459−467. (b) Tran, P. B.; Miller, R. J. Chemokine receptors: signposts to brain development and disease. *Nature Rev. Neurosci.* **2003**, *4*, 444−455. (c) Mennicken, F.; Maki, R.; de Souza, E. B.; Quirion, R. Chemokines and chemokine receptors in the CNS: a possible role in neuroinflammation and patterning. *Trends Pharmacol. Sci.* **1999**, *20*, 73−78. (d) Proudfoot, A. E. I. Chemokine receptors: multifaceted therapeutic targets. *Nature Rev. Immunol.* **2002**, *2*, 106−115.

(18) Kazmierski, W. M.; Aquino, C.; Chauder, B. A.; Deanda, F.; Ferris, R.; Jones-Hertzog, D. K.; Kenakin, T.; Koble, C. S.; Watson, C.; Wheelan, P.; Yang, H.; Youngman, M. Discovery of Bioavailable 4,4-Disubstituted Piperidines as Potent Ligands of the Chemokine Receptor 5 and Inhibitors of the Human Immunodeficiency Virus-1. *J. Med. Chem.* **2008**, *51*, 6538−6546.

(19) Li, G.; Wang, D.; Sun, M.; Li, G.; Hu, J.; Zhang, Y.; Yuan, Y.; Ji, H.; Chen, N.; Liu, G. Discovery and Optimization of Novel 3-Piperazinylcoumarin Antagonist of Chemokine-like Factor 1 with Oral Antiasthma Activity in Mice. *J. Med. Chem.* **2010**, *53*, 1741−1754.

(20) Forbes, I. T.; Cooper, D. G.; Dodds, E. K.; Hickey, D. M. B.; Ife, R. J.; Meeson, M.; Stockley, M.; Berkhout, T. A.; Gohil, J.; Groot, P. H. E.; Moores, K. CCR2B receptor antagonists: conversion of a weak HTS hit to a potent lead compound. *Bioorg. Med. Chem. Lett.* **2000**, *10*, 1803−1806.

(21) Gao, Z.; Metz, W. A. Unraveling the Chemistry of Chemokine Receptor Ligands. *Chem. Rev.* **2003**, *103*, 3733−3752.

(22) Bizzarri, C.; Beccari, A. R.; Bertini, R.; Cavicchia, M. R.; Giorgini, S.; Allegretti, M. ELR+ CXC chemokines and their receptors (CXC chemokine receptor 1 and CXC chemokine receptor 2) as new therapeutic targets. *Pharmacol. Ther.* **2006**, *112*, 139−149.

(23) Baxter, A.; Bennion, C.; Bent, J.; Boden, K.; Brough, S.; Cooper, A.; Kinchin, E.; Kindon, N.; McInally, T.; Mortimore, M.; Roberts, B.; Unitt, J. Hit-to-lead studies: the discovery of potent, orally bioavailable triazolethiol CXCR2 receptor antagonists. *Bioorg. Med. Chem. Lett.* **2003**, *13*, 2625−2628.

(24) (a) Baxter, A.; Cooper, A.; Kinchin, E.; Moakes, K.; Unitt, J.; Wallace, A. Hit-to-lead studies: the discovery of potent, orally bioavailable thiazolopyrimidine CXCR2 receptor antagonists. *Bioorg. Med. Chem. Lett.* **2006**, *16*, 960−963. (b) Hunt, F.; Austin, C.; Austin, R.; Bonnert, R.; Cage, P.; Christie, J.; Christie, M.; Dixon, C.; Hill, S.; Jewell, R.; Martin, I.; Robinson, D.; Willis, P. SAR studies on thiazolo[4,5-*d*]pyrimidine based CXCR2 antagonists involving a novel tandem displacement reaction. *Bioorg. Med. Chem. Lett.* **2007**, *17*, 2731−2734. (c) Walters, I.; Austin, C.; Austin, R.; Bonnert, R.; Cage, P.; Christie, M.; Ebden, M.; Gardiner, S.; Grahames, C.; Hill, S.; Hunt, F.; Jewell, R.; Lewis, S.; Martin, I.; Nicholls, D.; Robinson, D. Evaluation of a series of bicyclic CXCR2 antagonists. *Bioorg. Med. Chem. Lett.* **2008**, *18*, 798−803. (d) Bonnert, R.; Cage, P.; Hunt, F.; Jewell, R.; Walters, I. Preparation of thiazolopyrimidines as modulators of chemokine receptor activity. PCT Int. Appl. WO 2001058907, August 16 , 2001. (e) Willis, P. A.; Bonnert, R. V.; Hunt, S. F.; Walters, I. A. S. Preparation of novel thiazolo[4,5-*d*]pyrimidines as modulators of chemokine receptors. PCT Int. Appl. WO 2001025242 April 12, 2001. (f) Austin, R.; Baxter, A.; Bonnert, R.; Hunt, F.; Kinchin, E.; Willis, P. Preparation of novel thiazolopyrimidines as modulators of chemokine receptor activity. PCT Int. Appl. WO 2000009511, February 24, 2000. (g) Grahames, C.; Mallinder, P.; Mcintosh, F.; Tomkinson, N.; Wright, T. Screening for allosteric modulators of class A G protein-coupled receptors. PCT Int. Appl. WO 2006101439, September 28, 2006. (h) de Kruijf, P.; van Heteren, J.; Lim, H. D.; Conti, P. G. M.; van der Lee, M. M. C.; Bosch, L.; Ho, K.-K.; Auld, D.; Ohlmeyer, M.; Smit, M. J.; Wijkmans, J. C. H. M.; Zaman, G. J. R.; Smit, M. J.; Leurs, R. J. Nonpeptidergic allosteric antagonists differentially bind to the CXCR2 chemokine receptor. *Pharmacol. Exp. Ther.* **2009**, *329*, 783−790; and errata in **2009**, *330*, 367.

(25) Marumoto, R.; Yoshioka, Y.; Miyashita, O.; Shima, S.; Imai, K.; Kawazoe, K.; Honjo, M. Synthesis and coronary vasodilating activity of 2-substituted adenosines. *Chem. Pharm. Bull.* **1975**, *23*, 759−774.

(26) Brown, H. C.; Chandrasekharan, J.; Ramachandran, P. V. Chiral synthesis via organoboranes. 14. Selective reductions. 41. Diisopino-

campheylchloroborane, an exceptionally efficient chiral reducing agent. *J. Am. Chem. Soc.* **1988**, *110*, 1539−1546.
(27) (a) Masui, M.; Shioiri, T. A practical method for asymmetric borane reduction of prochiral ketones using chiral amino alcohols and trimethyl borate. *Synlett* **1997**, 273−274. (b) Ponzo, V. L.; Kaufman, T. S. A simple protocol for the one pot synthesis of chiral secondary benzylic alcohols by catalytic enantioselective reduction of aromatic ketones. *Synlett* **2002**, 1128−1130. (c) Corey, E. J.; Helal, C. J. Reduction of carbonyl compounds with chiral oxazaborolidine catalysts: a new paradigm for enantioselective catalysis and a powerful new synthetic method. *Angew. Chem., Int. Ed.* **1998**, *37*, 1986−2012.
(28) Waring, M. J. Defining optimum lipophilicity and molecular weight ranges for drug candidates—molecular weight dependent lower log *D* limits based on permeability. *Bioorg. Med. Chem. Lett.* **2009**, *19*, 2844−2851.
(29) Obach, R. S.; Lombardo, F.; Waters, N. J. Trend analysis of a database of intravenous pharmacokinetic parameters in humans for 670 drug compounds. *Drug Metab. Dispos.* **2008**, *36*, 1385−1405.
(30) Minagar, A.; Alexander, S. J. Blood−brain barrier disruption in multiple sclerosis. *Mult. Scler.* **2003**, *9*, 540−549.
(31) Most of the compounds have been disclosed in the patent literature: (a) Hanson, S.; Nordvall, G. Thiazolopyrimidine derivatives and use thereof as antagonists of the CX_3CR1 receptor. PCT Int. Appl. WO 2002076990, October 3, 2002. (b) Nordvall, G.; Rein, T.; Sohn, D.; Zemribo, R. New 2-substituted-4-amino-thiazolo[4,5-*d*]-pyrimidines, useful as chemokine receptor antagonists, esp. CX3CR1. PCT Int. Appl. WO 2005033115, April 14, 2005. (c) Nordvall, G.; Ray, C.; Rein, T.; Sohn, D. Preparation of 5,7-disubstituted thiazolo[4,5-*d*]pyrimidin-2(3*H*)-ones as chemokine CX3CR1 receptor antagonists. PCT Int. Appl. WO 2006107257, October 12, 2006. (d) Nordvall, G.; Ray, C.; Rein, T.; Sohn, D. Preparation of 5-substituted 7-aminothiazolo[4,5-*d*]pyrimidines as chemokine CX3CR1 receptor antagonists. PCT Int. Appl. WO 2006107258, October 12, 2006. (e) Johansson, R.; Karlstroem, S.; Kers, A.; Nordvall, G.; Rein, T.; Slivo, C. Preparation of [(pyridinyl)-ethyl]thio[(hydroxymethyl)alkyl]amino[1,3]thiazolo[4,5-*d*]-pyrimidinone derivatives for use as therapeutic agents. PCT Int. Appl. WO 2008039138, April 3, 2008. (f) Johansson, R.; Karlstroem, S.; Kers, A.; Nordvall, G.; Rein, T.; Slivo, C. Preparation of novel 5,7-disubstituted [1,3]thiazolo[4,5]pyrimidin-2(3*H*)-amine derivatives and their use in therapy. PCT Int. Appl. WO 2008039139, April 3, 2008.
(32) Harrington, C. R. Lowry protein assay containing sodium dodecyl sulfate in microtiter plates for protein determinations on fractions from brain tissue. *Anal. Biochem.* **1990**, *186*, 285−287.
(33) Kerns, E. H.; Di, L.; Carter, G. T. In vitro solubility assays in drug discovery. *Curr. Drug Metab.* **2008**, *9*, 879−885.
(34) Neuhoff, S.; Ungell, A.-L.; Zamora, I.; Artursson, P. pH-Dependent Bidirectional Transport of Weakly Basic Drugs Across Caco-2 Monolayers: Implications for Drug−Drug Interactions. *Pharm. Res.* **2003**, *20*, 1141−1148.
(35) Sohlenius-Sternbeck, A.-K.; Afzelius, L.; Prusis, P.; Neelissen, J.; Hoogstraate, J.; Johansson, J.; Floby, E.; Bengtsson, A.; Gissberg, O.; Sternbeck, J.; Petersson, C. Evaluation of the human prediction of clearance from hepatocyte and microsome intrinsic clearance for 52 drug compounds. *Xenobiotica* **2010**, *40*, 637−649.
(36) Floby, E.; Johansson, J.; Hoogstraate, J.; Hewitt, N. J.; Hill, J.; Sohlenius-Sternbeck, A.-K. Comparison of intrinsic metabolic clearance in fresh and cryopreserved human hepatocytes. *Xenobiotica* **2009**, *39*, 656−662.
(37) Briem, S.; Martinsson, S.; Bueters, T.; Skoglund, E. Combined approach for high-throughput preparation and analysis of plasma samples from exposure studies. *Rapid Commun. Mass Spectrom.* **2007**, *21*, 1965−1972.
(38) Cosimelli, B.; Greco, G.; Ehlardo, M.; Novellino, E.; Da Settimo, F.; Taliani, S.; La Motta, C.; Bellandi, M.; Tuccinardi, T.; Martinelli, A.; Ciampi, O.; Trincavelli, M. L.; Martini, C. Derivatives of 4-Amino-6-hydroxy-2-mercaptopyrimidine as Novel, Potent, and Selective A3 Adenosine Receptor Antagonists. *J. Med. Chem.* **2008**, *51*, 1764−1770.